Available online at www.sciencedirect.com
ScienceDirect
Estuarine, Coastal and Shelf Science 77 (2008) 549–564
ESTUARINE COASTAL AND SHELF SCIENCE
www.elsevier.com/locate/ecss

The relative contribution of processes driving variability in flow, shear, and turbidity over a fringing coral reef: West Maui, Hawaii

Curt D. Storlazzi*, Bruce E. Jaffe

U.S. Geological Survey, Pacific Science Center, 400 Natural Bridges Drive, Santa Cruz, CA 95060, USA

Received 17 October 2007; accepted 18 October 2007
Available online 30 October 2007

Abstract

High-frequency measurements of waves, currents and water column properties were made on a fringing coral reef off northwest Maui, Hawaii, for 15 months between 2001 and 2003 to aid in understanding the processes governing flow and turbidity over a range of time scales and their contributions to annual budgets. The summer months were characterized by consistent trade winds and small waves, and under these conditions high-frequency internal bores were commonly observed, there was little net flow or turbidity over the fore reef, and over the reef flat net flow was downwind and turbidity was high. When the trade winds waned or the wind direction deviated from the dominant trade wind orientation, strong alongshore flows occurred into the typically dominant wind direction and lower turbidity was observed across the reef. During the winter, when large storm waves impacted the study area, strong offshore flows and high turbidity occurred on the reef flat and over the fore reef. Over the course of a year, trade wind conditions resulted in the greatest net transport of turbid water due to relatively strong currents, moderate overall turbidity, and their frequent occurrence. Throughout the period of study, near-surface current directions over the fore reef varied on average by more than 41° from those near the seafloor, and the orientation of the currents over the reef flat differed on average by more than 65° from those observed over the fore reef. This shear occurred over relatively short vertical (order of meters) and horizontal (order of hundreds of meters) scales, causing material distributed throughout the water column, including the particles in suspension causing the turbidity (e.g. sediment or larvae) and/or dissolved nutrients and contaminants, to be transported in different directions under constant oceanographic and meteorologic forcing.
Published by Elsevier Ltd.

Keywords: coral reefs; waves; tides; currents; turbidity; shear; USA; Hawaii; Maui

1. Introduction

Coral reefs typically grow in relatively clear, oligotrophic waters. Land use practices such as overgrazing and coastal development can increase the supply of terrestrial sediment to the nearshore. Fine-grained terrestrial sediment can increase turbidity, which in turn, decreases light available for photosynthesis and can create physiological stress or even coral mortality (Marszalek, 1981; Buddemeier and Hopley, 1988; Acevedo et al., 1989; Fortes, 2000). The syntheses by Rogers (1990) and Fabricius (2005) noted that the magnitude and duration of sediment and turbidity play a significant factor in the ecological response of both individual corals and coral reef ecosystems.

Most coral reef sampling protocols (e.g. Devlin and Lourey, 2000) and scientific studies investigating the influence of land-based material on nearshore coral reefs have employed limited sampling schemes over the course of a day(s) or tidal cycle(s); these data are then often used by regulatory agencies (e.g. State of Hawaii, 2004) to determine if specific water bodies meet defined water quality standards. A number of recent studies, however, suggest that flow and water column properties over a reef flat vary temporally (Ogston et al., 2004) and those over a fore reef are spatially heterogeneous (Storlazzi et al., 2006b). While a number of investigations have focused on

* Corresponding author.
E-mail addresses: cstorlazzi@usgs.gov (C.D. Storlazzi), bjaffe@usgs.gov (B.E. Jaffe).

0272-7714/$ - see front matter Published by Elsevier Ltd.
doi:10.1016/j.ecss.2007.10.012

wave-, wind- or tidally-driven flow and transport along or across a reef (e.g. Roberts et al., 1980; Wolanski and Delesalle, 1995; Kraines et al., 1998; Lugo-Fernandez et al., 1998; Tartinville and Rancher, 2000; Leichter et al., 2003; Storlazzi et al., 2004; Lowe et al., 2005), most of these investigations have been limited in duration to the course of a few weeks to a few months and thus the contribution of the observed mechanisms driving flow and transport to annual budgets was not constrained.

This paper addresses the nature of flow and water column properties on the fringing reef of Kahana, northwest Maui, over a range of seasons. An experiment was designed with the goal to better understand the controls on hydrographic variability along a relatively geometrically-simple fringing reef and determine the contribution of these different processes to annual budgets. The observations described here elucidate the complex interactions between the wind, waves, tides, high-frequency motions, and lower-frequency currents that drive significant spatial and temporal variations in flow and turbidity off northwest Maui.

2. Study area

The island of Maui, Hawaii, USA, is located at 20.8° N, 156.5° W in the north-central Pacific between the islands of Molokai, Lanai, and Hawaii (''the Big Island'') in the Hawaiian Archipelago (Fig. 1). The northwest Maui coastline is characterized by a series of sandy beaches, fringing reefs and a sandy insular shelf. Over the past two decades, a number of factors have affected the quality of the nearshore waters off northwest Maui. Coastal development and agriculture have increased runoff and the supply of sediment to northwest Maui's coastal waters, while terrestrial wastewater injection has increased the volume of nutrients percolating out of the shoreface via submarine groundwater discharge (Soicher and Peterson, 1996; West Maui Watershed Management Project, 1996; De Carlo and Dollar, 1997; Dollar and Andrews, 1997).

2.1. Geology

Maui is comprised of two large basaltic shield volcanoes that formed in the last 2 million years (Clague and Dalrymple, 1989) and are separated by a flat isthmus. Western Maui is roughly 30 km long in the north-south direction and on average 20 km wide in the east-west direction. Land use in the study area was historically dominated by pineapple and sugarcane cultivation; more recently, however, urbanization and development along the shoreline have increased substantially (M&E Pacific, 1991).

The shoreline in the study area is characterized by small basaltic headlands, carbonate sand beaches and a few small, ephemeral stream mouths that drain coastal development and upland pineapple fields. The geomorphology of the inner shelf (<40 m depth) off northwest Maui in the Pailolo Channel between the islands of Maui and Molokai is highly variable and includes boulders, small patches of sand, extensive sand fields and a number of fringing coral reefs as discussed by Gibbs et al. (2005). The fringing reef along this stretch of coast extends from the shoreline out to 1 km offshore in water depths of 25–30 m and approximately 6 km alonghsore.

The inner portion of the reef flat is covered by a wedge of muddy sand (most of the silt and clay is composed of reddish-brown terrigenous particles) that pinches out within 100 m from shore. From this point out to the reef crest, approximately 600 m offshore, the reef flat is characterized by depressions filled with fine to coarse calcareous sand and an ancestral reefal hardground covered by algae and low percentages of live coral. The reef crest is poorly defined along most of the reef off northwest Maui and is predominately covered by robust lobe corals, encrusting corals, and coralline algae. Offshore of the reef crest, from depths of 3 m to 25 m, lies the fore reef, which is characterized by 1–3 m high irregularly-shaped reefal hardgrounds. These hardgrounds are covered by algae and discontinuous, highly variable percentages of live coral (0–80%; Jokiel et al., 2001). The sediment on the fore reef is a well-sorted, coarsely-skewed clean white carbonate sand.

2.2. Oceanography and meteorology

The wave climate off northwest Maui is dominated by three end-members: North Pacific swell, Northeast trade wind waves and Southern Ocean swell (Moberly and Chaimberlin, 1964). The North Pacific swell is generated by strong winter storms as they track from west to east across the North Pacific, typically in the winter between November and March, generating significant wave heights generally between 3 and 8 m and dominant periods on the order of 10–20 s. The Northeast trade wind waves occur throughout the year but are largest from April through November when the trade winds are the strongest (Western Region Climate Center, 2006); these waves have significant heights typically between 1 and 4 m and dominant periods on the order of 5–8 s. The Southern swell is generated by storms in the Southern Ocean during the Southern Hemisphere winter and although typical significant wave heights are small (~1–2 m), these waves have long periods (dominant periods ~14–25 s).

The Northeast trade winds strike the northeast side of West Maui, are steered around the West Maui volcanic cone and most often approach the Kahana shoreline obliquely from the north. Due to orographic effects associated with the high (>1400 m) West Maui shield volcano, most of the precipitation (100–400 cm/year) falls on the northern face of the volcano while the south and southwest sides of the volcano receive less than 40 cm/year on average (Fletcher et al., 2002). This causes a north-south gradient in both stream flow and terrestrial sediment discharge into the study area, with greater freshwater and sediment discharge to the north of Kahana than to the south. Most of the lower portions of the streams are intermittent in nature, leaving the stream beds dry during most of the year with stream flow at the lower elevations occurring only during periods of heavy rain, typically in winter months (Soicher and Peterson, 1996).

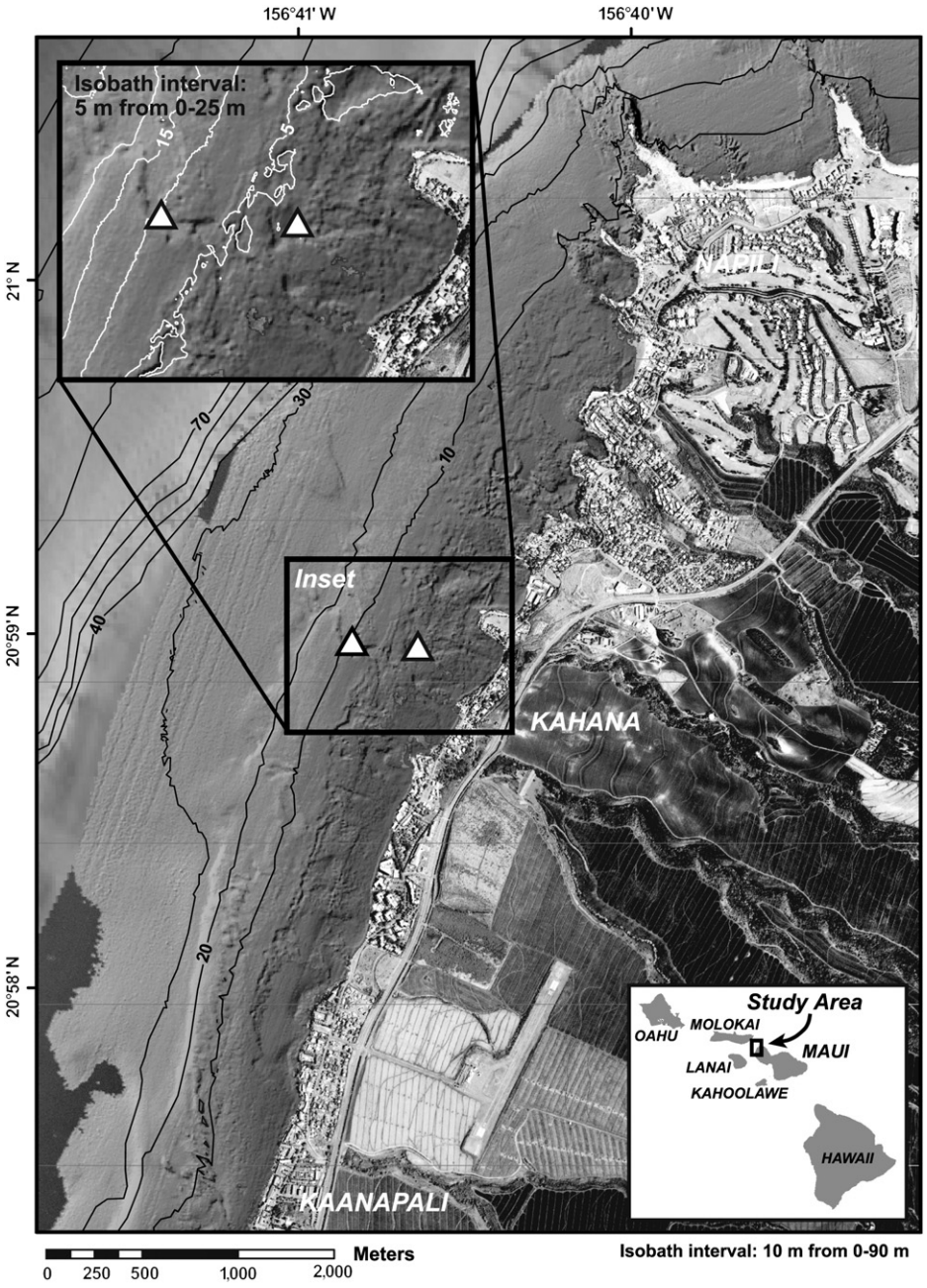

Fig. 1. Maps showing the location of the instrument packages relative to the morphology of the study area. NOAA aerial image showing the terrestrial landscape and the location of major drainages; the bathymetry was developed from SHOALS LiDAR and USGS multibeam data.

3. Field experiment and methods

Two primary instruments were used to acquire data during these field deployments. The first instrument was a 600 kHz upward-looking acoustic Doppler current profiler (ADCP). The second primary instrument employed was a downward-looking 5 MHz acoustic Doppler current velocimeter (ADV). A logger collected and stored data from the ADV and four external sensors: a pressure sensor, a conductivity-temperature sensor and two 880-nm optical backscatter sensors (OBS). Both of these instruments were mounted on the REEFPROBE tripod that was deployed in a sand patch along the 10 m isobath on the fore reef off Kahana between November 2001 and February 2003 (Storlazzi and Jaffe, 2003). Nine months into the 15-month experiment, the smaller MiniPROBE package was deployed in a 2 m deep hole on the reef flat along the 2 m isobath (total depth ~4 m) 350 m inshore of the REEFPROBE instrument package; it had a 600 kHz upward-looking ADCP similar to the one on the deeper REEFPROBE tripod and a self-logging 880-nm OBS.

The instrument packages were typically deployed for 90–100-day periods, as constrained by the power consumption. The logger on the REEFPROBE tripod collected data from all sensors each hour to determine water depth, currents,

wave heights, wave periods and wave direction, along with salinity, temperature, and acoustic backscatter. The upward looking ADCPs mounted on the REEFPROBE tripod and the MiniPROBE sampled every 4 min to measure water depth, temperature, and vertical profiles of currents and acoustic backscatter. Cross-shore and alongshore directions are defined relative to the general orientation of the isobaths and shoreline, which trend 30–210°; positive alongshore is defined upwind to the northeast. See Table 1 for information on the instrumentation and sampling schemes. Meteorologic data were obtained from the National Climate Data Center's (NCDC, 2004) Kahului Airport Station (ID# 22516), approximately 25 km to the east of the study area. Sediment tube traps, with their openings 0.6 m above the bed (mab), were attached to both instrument packages during the last deployment (November 2002 to January 2003) to capture suspended sediment for analysis. The tube traps were 60 cm long and had an internal diameter of 6.7 cm; a hexagonal baffle (cells 0.5 cm diameter, 7.6 cm long) consisting of phenolic resin and treated with anti-fouling paint was placed in the top of the trap to reduce turbulence and prevent occupation by fish or crustaceans. The trap design and sample processing followed the methodology of Bothner et al. (2006).

It is relatively simple to calculate suspended sediment concentration in units of mass per volume from single-wavelength optical or acoustic measurements in homogeneous sedimentary environments using sediment samples collected in the field (e.g. Larcombe et al., 1995). These optical and acoustic sensors, however, suffer from calibration changes when particle size and particle composition (e.g. color) vary. Laser In-Situ Scattering and Transmissometry (LISST) data collected in 2003 (J. Harney, personal communication) showed that both the composition and grain size of suspended sediment varied both spatially and temporally in the study area, with both white carbonate sands and reddish-brown terrestrial mud being observed.

The mixed grain size environment off west Maui made it impossible to accurately calculate suspended sediment concentration is units of mass per volume and thus only measurements of turbidity are presented here. The OBSs were calibrated to Nephelometric Turbidity Units (NTUs) using 5 (0, 10, 50, 100 and 200 NTU) formazin calibration standards. These NTU values from the OBSs were then correlated to co-located acoustic backscatter data recorded by the ADV and ADCPs that had been corrected for signal strength decay with distance from the transducers due to spreading and absorption using the method outlined by Deines (1999). This method has been used successfully for quantitative measurements of suspended sediment concentrations in numerous studies (e.g. Thorne et al., 1991; Osborne et al., 1994; Reichel and Nachtnebel, 1994; Holdaway et al., 1999). The correlations between the ADCPs' and ADV's corrected acoustic backscatter and the co-located, unfouled OBS data had r^2 correlations of 0.64 ($n = 3128$) and 0.81 ($n = 1051$), respectively; these correlations are significant above the 0.1% level. We define turbidity flux as the product of the flow velocity (m/s) and turbidity (NTU) and utilize it as a proxy for the physical transport of particles that create optical backscatter and thus turbidity. Because the turbidity/mass ratio is greater for finer particles, and the ratio of fine to coarse particles in suspension varies spatially and temporally, it is not possible to directly infer mass flux from our measurements. Please see Storlazzi and Jaffe (2003) for more details on instrumentation, data acquisition and processing methodology.

4. Results

Data were acquired on 429 days during the 15-month period between December 5, 2001 and 27 February, 2003; this was more than 96% data coverage over the entire experiment. The results are presented to address variability at two relative time scales: (a) variability between seasons; and (b) variability within seasons.

4.1. Summer

The summer–early fall regime is dominated by the northernmost position of the Pacific High, which brings the heart

Table 1
Instrumentation and sampling schemes during the experiment

Instrument	Depth (m)	Instruments	Elevation (m)	Sampling rate (s)	Burst length (s)	Burst interval (s)
REEFPROBE	10	Acoustic Doppler velocimeter	0.2	0.5	512	3600
		Pressure sensor	1.0	0.5	512	3600
		Salinity sensor	1.0	0.5	512	3600
		Optical backscatter sensor	0.2	0.5	512	3600
		Optical backscatter sensor	1.0	0.5	512	3600
		Acoustic Doppler current profiler	2.0–10.0 every 1.0	0.25	40	240
		Temperature sensor	1.0	0.25	40	240
MiniPROBE	4	Acoustic Doppler current profiler	1.0–4.0 every 0.5	0.25	40	240
		Temperature sensor	0.2	0.25	40	240
		Optical backscatter sensor	0.2	0.5	15	240
		Pressure sensor	0.2	0.5	512	3600

of the trade winds across the Hawaiian Islands. This period is characterized by consistent northeast trade winds (prevalent 80–95% of the time; Western Region Climate Center, 2006) and small trade wind waves (Fig. 2). All across the fringing reef, the currents were primarily alongshore and their magnitude was strongly influenced by the tides, similar to the observations by Storlazzi et al. (2004) over the fringing reef off southern Molokai, Hawaii. In general, the currents show less coherence with the tides 0.2 mab over the fore reef and 1.0 mab on the reef flat than 6.0 mab over the fore reef, likely due to hydrodynamic roughness of the seafloor. The mean difference in direction between near-surface currents and near-bed currents over the fore reef was $32.8 \pm 33.0°$, while the mean difference in direction between currents over the fore reef and those on the reef flat was $65.2 \pm 53.1°$.

During this time period the turbidity was always greatest 0.2 mab and lowest 6.0 mab over the fore reef; turbidity 1.0 mab on the reef flat was always greater than 6.0 mab over the fore reef. Turbidity 6.0 mab over the fore reef increased with offshore-directed currents and falling tides, similar to the observations made off the south Molokai fringing reef (Storlazzi et al., 2004). At 0.2 mab on fore reef however, turbidity increased with increasing tidal elevation, opposite what was seen at 6.0 mab; turbidity at 0.2 mab over the fore also increased with wave height but was not correlated with the currents. Turbidity at 1.0 mab over the reef flat increased with higher tidal elevations, wind speeds, wave heights and both offshore-directed and alongshore currents downwind to the southwest; Ogston et al. (2004) made similar observations of turbidity over the south Molokai reef flat. All across the reef, water temperature was positively correlated with falling tides and offshore-directed currents; while all significant, these correlations explained more of the variance high up in the water column over the fore reef than closer to the bed or on the reef flat.

Two distinct events during this time period show the typical modification of these general low-frequency trends. During the period of Year Day 2002 (YD) 266–271 and YD 287–291 (Fig. 2), propagation of atmospheric fronts to the north of the study area caused the northeast trade winds to weaken and be replaced by southerly winds. These periods were marked by higher variance in the subtidal flow field all across the reef and slightly elevated turbidity over the fore reef. In contrast, turbidity over the reef flat was slightly less during these events than otherwise in the summer/early fall period.

A 5-day time series of sub-tidal (>36 h) low-pass filtered alongshore wind velocity, water level, alongshore current velocity, turbidity and water temperature during a period of relatively consistent wave forcing displays the influence of wind on fore reef and reef flat processes (Fig. 3). As the trade winds began to wane, the alongshore wind velocity to the southwest decreased below 6 m/s, the water level began to drop, and the alongshore currents shifted from southwestward (downwind) to northeastward flow. The currents over the fore reef appeared to responding more rapidly to the reduction in alongshore winds than those over the reef flat, which did not change substantially until YD 288. Concurrently with this decrease in alongshore flow to the southwest, turbidity decreased and temperature began to increase over both the fore reef and reef flat. These data suggest that some type of large-scale relaxation may occur when the trade winds decrease in strength, with the warmer, less turbid water in the channels between Maui, Molokai, Lanai and Kahoolawe flowing northwestward out through the Pailolo Channel. These flows may be due to the passage of an island-trapped wave (ITW), as observed by Flament and Lumpkin (1996) and modeled by Merrifield et al. (2002).

Roughly once per day when the trade winds blew consistently and wave heights were small, a very rapid (typically <16–32 min) change in temperature was often observed at the fore reef site; an example of one of these events is shown in Fig. 4. The water temperature typically changed by more than 0.5 °C and frequently by more than 1.0 °C in as little as 8 min (mean = 16 min) and these events had a mean duration of 104 min. These rapid changes in water temperature occurred during all but the spring phases (new and full moon) of the fortnightly tidal cycle and during all phases (low, rising, high and falling) of the diurnal tidal cycle. Almost all of these features were preceded by cross-shore shear in the water column (typically >0.02 1/s) and vertical gradients in turbidity. At the time of the rapid change in water temperature, the flow in the water column would always rapidly switch direction, with onshore near-surface flow changing to offshore near-surface flow and near-bed offshore flow changing to onshore near-bed flow, or vice versa; these typically coincided with changes in the vertical turbidity gradient, often resulting in inverted turbidity profiles (higher turbidity near the surface than near the seabed). These rapid changes in water temperature and flow directions were followed by cyclical variations in flow, temperature and turbidity. A rapid warming typically occurred when near-surface waters moved onshore and near-bed waters moved offshore while rapid cooling typically occurred when near-surface waters moved offshore and near-bed waters moved onshore. These features showed similar structure to internal tidal bores observed elsewhere on coral reefs (Wolanski and Delesalle, 1995; Leichter et al., 2003).

4.2. Winter

During the winter months, the Hawaiian Islands are located to the north of the heart of the trade winds. The trades still blow across the islands much of the wintertime, though less regularly (50–80% of the time; Western Region Climate Center, 2006). Major storms occur most frequently during this period, often bringing heavy rain, strong winds and large waves (Fig. 5). Cold fronts and low-pressure systems, known locally as Kona storms, bring heavy rains, often accompanied by strong winds and large waves from directions other than that of the northeast trade winds. While the seafloor sediment is a well-sorted, coarsely-skewed clean carbonate sand at both instrument locations and the coarse-grained (>62.5 μm) sediment collected in both sediment traps during this period was relatively clean whitish carbonate sand (>74% carbonate), the fine-grained component (<62.5 μm) in both traps was

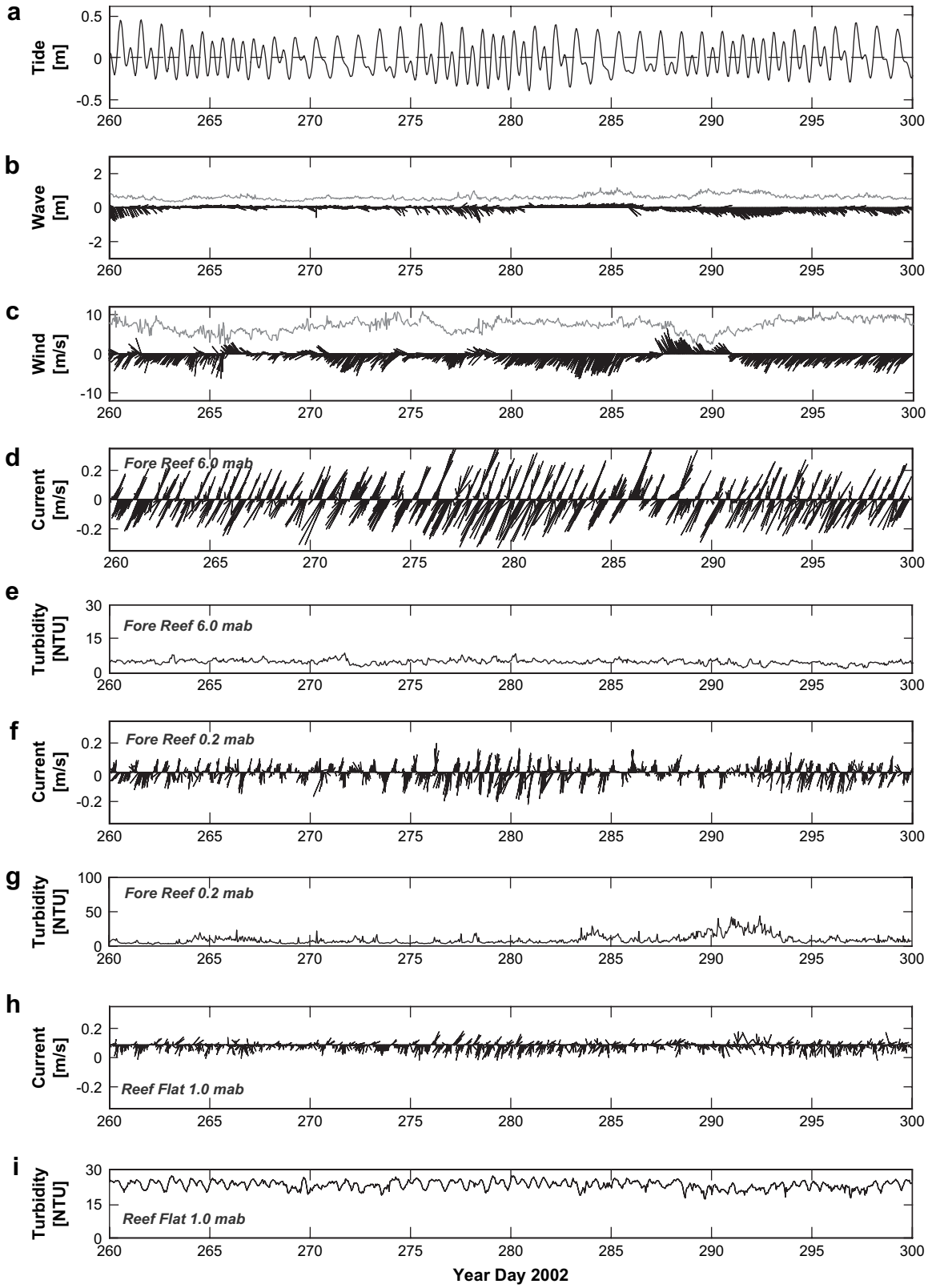

Fig. 2. Example of the variability in hourly forcing and the water column's response during the quiescent early fall months. (a) Tide. (b) Wave height (gray) and magnitude and direction (black). (c) Wind speed (gray) and magnitude and direction (black; NCDC, 2004). (d) Current speed and direction 6.0 mab on the fore reef. (e) Turbidity 6.0 mab on the fore reef. (f) Current speed and direction 0.2 mab on the fore reef. (g) Turbidity 0.2 mab on the fore reef. (h) Current speed and direction 1.0 mab on the reef flat. (i) Turbidity 2.0 mab on the reef flat. Note the varying scales on the *y*-axes.

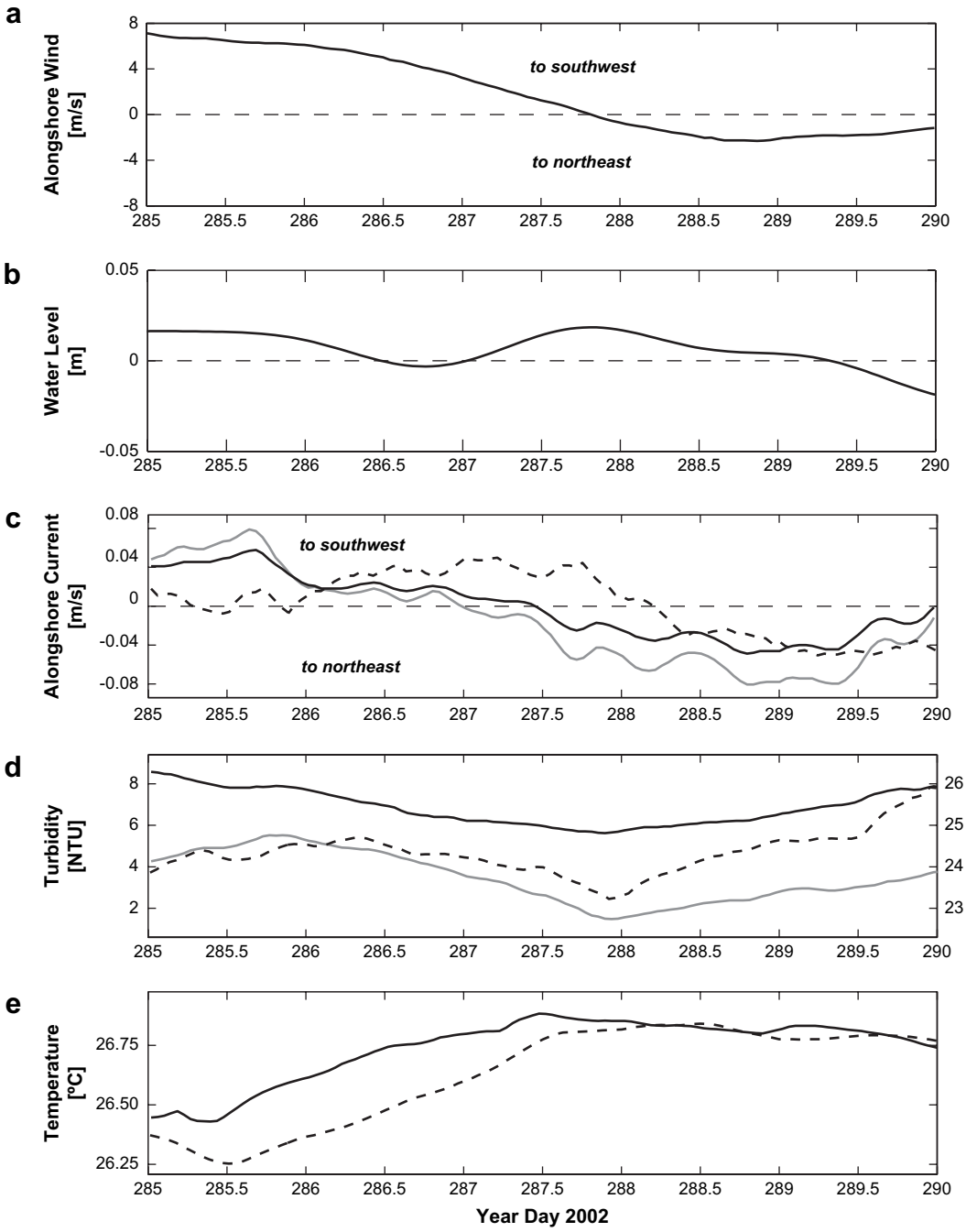

Fig. 3. Thirty-six hour low-pass filtered time series data showing the influence of alongshore wind forcing on sub-tidal water level, flow and water column properties over the fore reef. (a) Alongshore wind stress (NCDC, 2004). (b) Water depth. (c) Alongshore currents 2.0 mab (black) and 8.0 mab (gray) over the fore reef and 1.0 mab on the reef flat (dashed). (d) Turbidity 2.0 mab (black) and 8.0 mab (gray) over the fore reef and 1.0 mab on the reef flat (dashed; values on second *y*-axis). (e) Water temperature 1.0 mab over the fore reef (black) and 1.0 mab on the reef flat (dashed).

primarily (>68%) reddish terrigenous mud and contained numerous (>4%) organic particles.

In contrast to the more quiescent late summer and early fall months (Fig. 2), both the currents and the turbidity all across the fringing reef were less coherent with the tides. The mean variation in direction between near-surface currents and near-bed currents over the fore reef during the winter was approximately 43% greater ($47.2 \pm 46.5°$) than in the summer and early fall, while the mean variation in direction between currents over the fore reef and those on the reef flat was approximately 26% less ($48.2 \pm 49.5°$). When storms pass through the Hawaiian Islands and cause winds to blow from a direction other than their typical northeasterly orientation, the southwest-northeast oscillating tidal currents that characterize flow over the reef are replaced by strong net flows to the northeast. These storms also bring larger than normal waves to the study area, and turbidity all across the fringing reef during large wave events was more coherent with wave

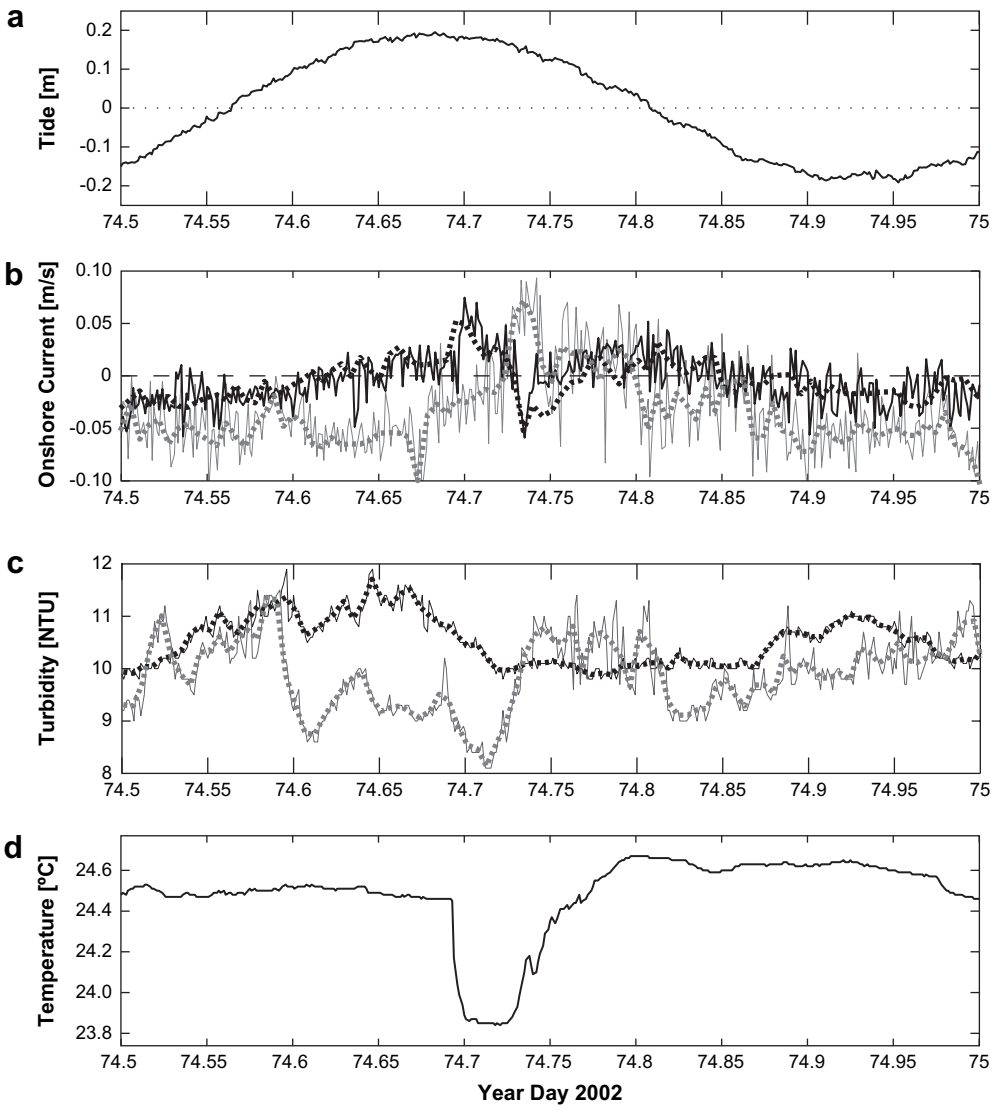

Fig. 4. Time series data showing the influence of high-frequency vertical velocity shear on flow and water column properties over the fore reef. (a) Tide. (b) Cross-shore currents 2.0 mab (black) and 8.0 mab (gray). (c) Turbidity 2.0 mab (black) and 8.0 mab (gray). (d) Water temperature 1.0 mab. Solid lines are 4-min data; dotted lines are 20-min low-pass filtered data. These features show similar structure to high-frequency internal bores observed on the inner shelf at many locations around the globe.

height than with the tides. Turbidity was greater 0.2 mab on the fore reef than 6.0 mab over the fore reef or 1.0 mab on the reef flat during this time period. While turbidity over the fore reef was greater during this time period than during the more quiescent late summer and early fall months, turbidity over the reef flat, while reaching greater maximum values than during the late summer and early fall months, had lower mean and minimum values during the more energetic winter months. The cross-shore and alongshore currents explained more of the variance in turbidity over the fore reef during the winter than during the summer months, but the cross-shore currents still explained roughly twice the variance of the alongshore currents (23–50% vs. 5–27%). Cross-shore currents over the reef flat explained almost twice the variance in turbidity than during the summer and early fall months (43% vs. 26%), while during the winter months the alongshore currents were no longer significantly correlated with turbidity. While temperature and salinity remained uncorrelated with alongshore currents, cross-shore currents explained, on average, twice the variance in temperature and salinity than during the summer and early fall months.

To better constrain the influence of waves on flow over the fringing reef, two time periods with similar wind and tidal forcing were examined (Fig. 6). Under small wave conditions (mean $\pm$ 1σ significant wave heights = 0.56 $\pm$ 0.06 m at 359°) and relatively constant wind forcing during YD 270–272, the flow over the fore reef was primarily alongshore, with mean flow to the northeast, and an increasingly greater onshore component of flow closer to the bed. The greater onshore component of flow near the bed is possibly due to wave orbital asymmetry as the waves shoal up the fore reef or topographic steering of the currents by the local reef morphology; it is

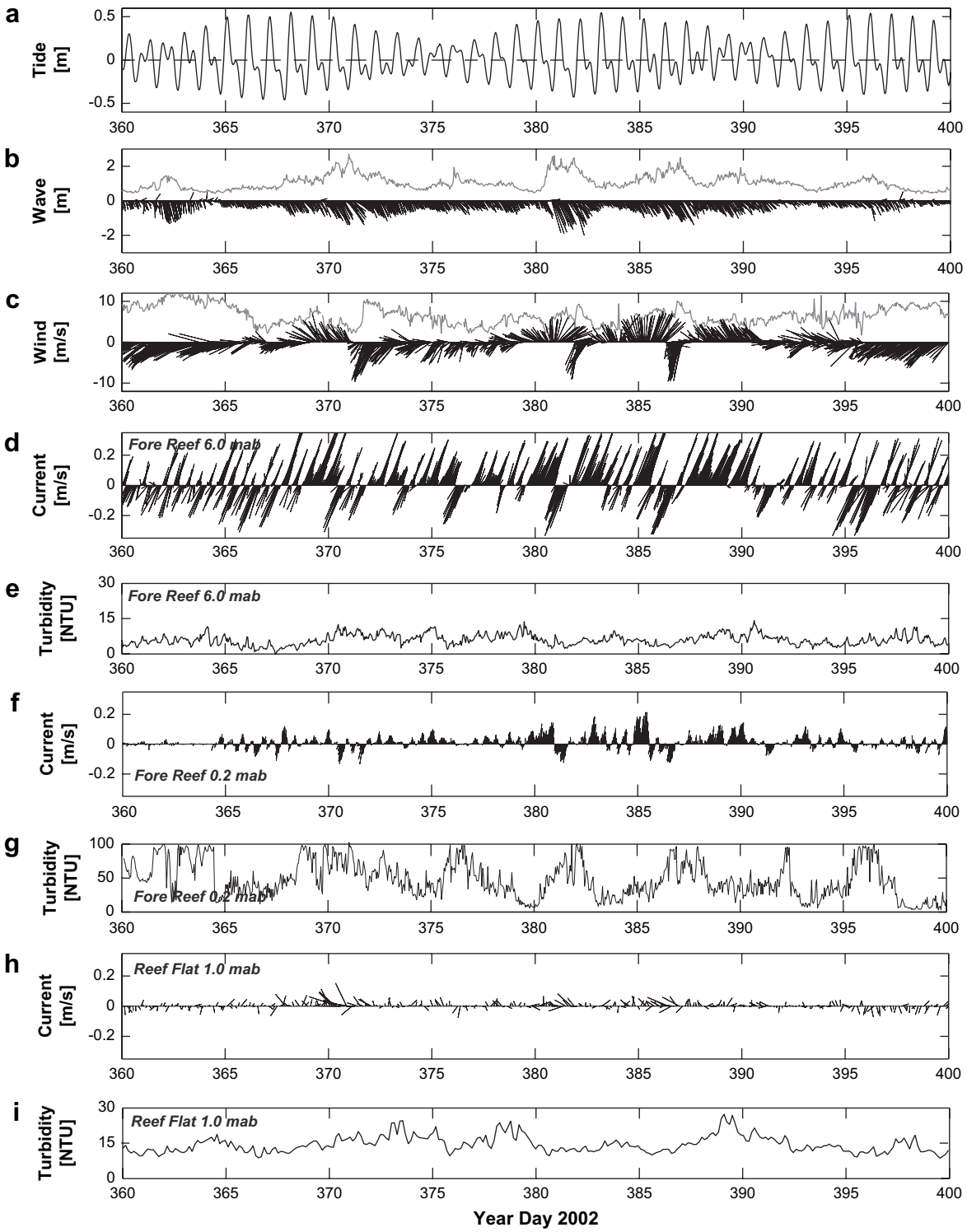

Fig. 5. Example of the variability in hourly forcing and the water column's response during the energetic winter months. (a) Tide. (b) Wave height (gray) and magnitude and direction (black). (c) Wind speed (gray) and magnitude and direction (black; NCDC, 2004). (d) Current speed and direction 6.0 mab on the fore reef. (e) Turbidity 6.0 mab on the fore reef. (f) Current speed and direction 0.2 mab on the fore reef. (g) Turbidity 0.2 mab on the fore reef. (h) Current speed and direction 1.0 mab on the reef flat. (i) Turbidity 2.0 mab on the reef flat. Note the varying scales on the *y*-axes.

not clear at this time which process or processes cause this on-shore flow. On the reef flat, however, the flow was more variable, with mean flow downwind to the southwest. Thus there was significant cross-shore velocity shear, with the mean flow over the fore reef heading upwind to the northeast and flow over the reef flat heading downwind to the south. Mean wind- and wind-driven wave flows downwind to the south over the reef flat and flow upwind to the northeast over

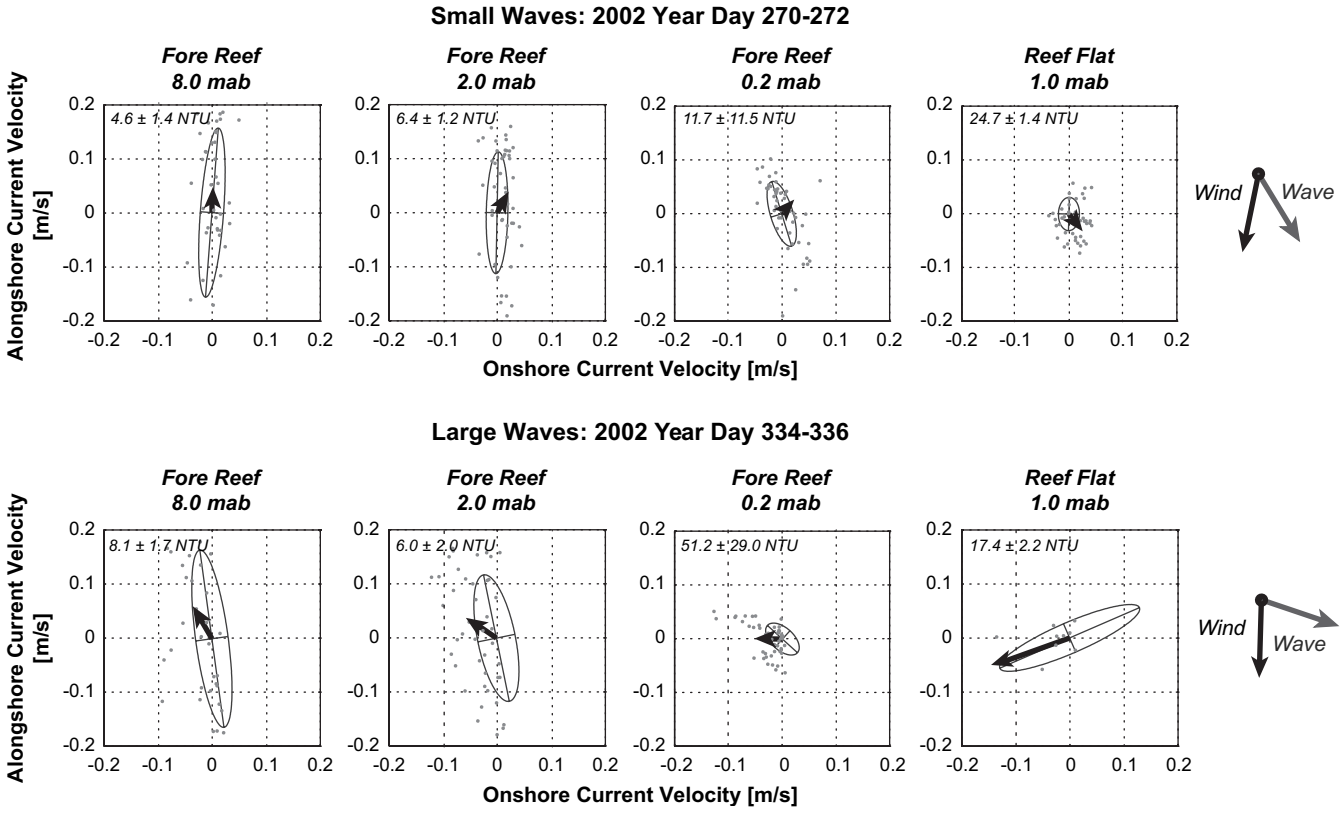

Fig. 6. Principal axes and mean current vectors showing the influence of large waves on flow across the reef. Top row (left to right): Currents 8.0 mab on the fore reef, 2.0 mab on the fore reef, 0.2 mab on the fore reef, and 1.0 mab on the reef flat during a period of small waves. Bottom row (left to right): Currents 8.0 mab on the fore reef, 2.0 mab on the fore reef, 0.2 mab on the fore reef, and 1.0 mab on the reef flat during a period of large waves. Positive alongshore is defined upwind to the northeast. The principal axes and means for each subplot were generated from 48-hourly means of 4 min ensemble data.

the fore reef were often observed using a vessel-mounted, downward-looking ADCP in this area during the summer of 2003 (Storlazzi et al., 2006b); similar distinctions were observed over reefs in the Caribbean by Roberts et al. (1980).

Under large wave conditions (mean $\pm$ 1σ significant wave heights = 1.67 $\pm$ 0.58 m at 308°; maximum significant wave height >2.5 m), the mean flow out over the fore reef was upwind to the north and had a component of offshore flow, which increased close to the bed; variability in current direction was also greater throughout the water column over the fore reef during this time period. Most impressive, however, was the strong mean offshore flow on the reef flat, with almost no onshore flow observed 1.0 mab during this time period.

5. Discussion

Variations in flow and turbid water transport along the fringing reef off Kahana, northwest Maui, can be categorized by four sets of meteorologic and oceanographic conditions: trade winds, relaxation events, large wave events and storms. Trade wind periods, which occurred 71.1% of the year, are defined by strong (>5 m/s) alongshore winds to the southwest and small (<1 m) waves. Relaxation events, which occurred 16.5% of the year, are similarly characterized by small (<1 m) waves, but differ by having weaker (<5 m/s) winds to the southwest or winds to the northeast. Large wave events, which occurred 10.1% of the year, are defined by strong (>5 m/s) alongshore winds to the southwest and large (>1 m) waves. Storm periods, which occurred 2.3% of the year, are defined as a combination of large (>1 m) waves and weaker (<5 m/s) winds to the southwest or winds to the northeast, which occurred when storm systems propagated through the study area.

5.1. Trade winds

When trade wind conditions prevailed, currents over the fore reef were primarily oriented alongshore and dominated by the tides. Overprinted on this symmetric alongshore tidal flow was weak mean flow offshore and downwind to the southwest, with the mean flow closest to the bed oriented primarily offshore and the net flow higher up in the water column alongshore to the southwest (Fig. 7). Similar to conditions over the fore reef, currents on the reef flat were oriented alongshore and dominated by the tides. Mean flow over the reef flat was to the southwest and slightly onshore, similar to the orientation of the trade winds that are topographically steered around the West Maui volcano and strike the coastline along northwest Maui obliquely to the south.

Turbidity varied across the reef under consistent trade wind forcing but was strongly influenced by the tides and generally higher during falling tides. Close to the seafloor over the fore

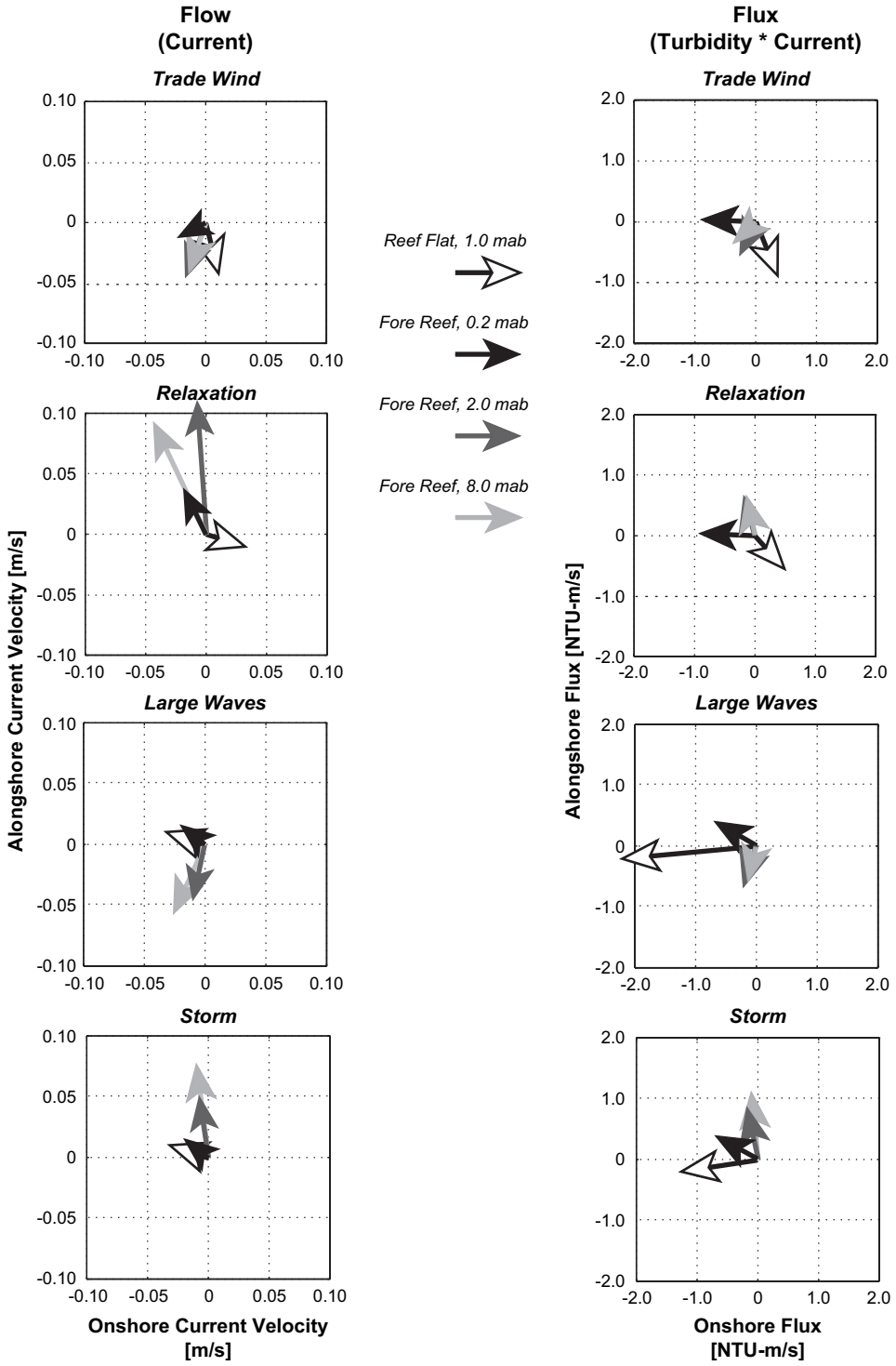

Fig. 7. Variability in mean flow (left column) and turbidity flux (right column), calculated as the product of the mean current velocity and mean turbidity, for different location across the reef and at different depths, under four combinations of meteorologic and oceanographic forcing. Top to bottom: Trade winds, defined by strong (>5 m/s) alongshore winds to the southwest and small (<1 m) waves; Relaxation events, defined by small (<1 m) waves and weaker (<5 m/s) winds to the southwest or winds to the northeast; Large Wave events, defined by strong (>5 m/s) alongshore winds to the southwest and large (>1 m) waves; and Storm periods, defined by large (>1 m) waves and weaker (<5 m/s) winds to the southwest or winds to the northeast. Positive alongshore is defined upwind to the northeast and the units are: m-NTU/s. Without coupling between currents and turbidity, the left column would look like the right column; the differences between the data in the two columns reflect the preferential phasing of certain orientations in flow and higher turbidity.

reef, the phasing of the currents and turbidity was such that the mean turbidity flux was oriented almost directly offshore. The near-surface turbidity flux over the fore reef, however, was oriented downwind to the southwest, showing more coherent phasing between the ebbing tidal currents and turbidity. Over the reef flat, the mean turbidity was much greater than out over the fore reef and was correlated to tidal elevation, similar to the observations by Ogston et al. (2004) and Presto

et al. (2006) over the reef flat off south Molokai. The data presented here suggest that the reef flat here is depth-limited, and greater trade wind-driven waves and wind-driven currents, and thus combined wave-current shear stresses, can develop at higher tidal elevations. Greater shear stresses appear to suspend greater volumes of seafloor sediment, which are then transported downwind by the trade wind-driven currents.

Water temperatures were more variable during trade wind periods, and the rapid changes in water temperature that appeared to be internal bores were consistently observed. Time series measurements of thermal stratification were not made by the instruments described in this study. Spatial surveys made in the study area during 2003 (Storlazzi et al., 2006b), however, showed thermal stratification, which is necessary for the formation and propagation of internal motions, to be greatest during periods of small waves and consistent trade wind forcing. While it is not clear if these internal motions observed over the fore reef are related to the deep internal tide generated by the interaction of the barotropic tide with the Hawaiian Ridge (Pinkel et al., 2000), similar internal bores have been shown to cause upwelling around islands (Wolanski and Delesalle, 1995) and episodically transport deep, subthermocline nutrients from offshore up onto the coral reefs in the Florida Keys (Leichter et al., 2003).

5.2. Relaxation

Unlike the nearly symmetric alongshore currents observed over the fore reef during trade wind periods, the currents during relaxation events were skewed to the northeast, sometimes to the point of having no flow to the southwest, even during the falling tide. Over the fore reef, mean flow during relaxation events was to the northeast throughout the water column (Fig. 7). On the reef flat, however, mean flow was relatively weak and oriented obliquely onshore to the southeast. This southeast mean flow on the reef flat, without concurrent wind forcing in the same orientation, suggests that these mean flows are driven by some other process, likely wave-orbital asymmetry as the waves shoal over the reef flat. The water generally warmed during these periods, likely due to the advection of warmer water from inside the Maui Nui complex northeastward past the study site.

Turbidity varied across the reef and was generally higher during falling tides, although it showed much less coherence with the tides than when the trade winds were steady. Turbidity just above the seafloor over the fore reef was slightly higher during relaxation events; further up in the water column over the fore reef and over the reef flat it was lower than during consistent trade winds. The lower turbidity on the reef flat during relaxation events further emphasizes the importance of the interaction between trade wind waves and currents on sediment resuspension on the depth-limited reef flat. The higher turbidity close to the bed over the fore reef, however, may be due to the slightly higher waves that often impact the study area when the low-pressure systems that cause the trade winds to wane pass the island chain. While flux high up in the water column over the fore reef and on the reef flat were aligned with the flow and headed to the north and southeast, respectively, the flux close to the bed was offshore to the west, showing significant correlation between offshore flow and high turbidity.

5.3. Large waves

During large wave events the currents were symmetric and oriented predominantly alongshore (Figs. 6 and 7). Close to the bed over the fore reef and up on the reef flat, the mean flow was oriented almost directly offshore, showing little influence of the tides. The offshore-directed mean flow over the reef flat compared to the downwind orientation of mean flow under trade winds and small waves suggests some type of offshore-directed, near-bed return flow balancing the wave-driven onshore surface flow up onto the reef by the larger waves, similar to the observations made over the fringing reef off south Molokai (Storlazzi et al., 2004) and modeled by Gourlay (1996). This return flow might also explain the greater magnitude of the mean flows higher up in the water column over the fore reef, which is approximately two times greater than under small wave conditions. The phasing of flow and turbidity were such that mean flux is oriented offshore, with the near-bed flux over the fore reef and up on the reef flat oriented almost directly offshore. The mean flux higher up in the water column over the fore reef, while oriented offshore, shows greater coherence between alongshore flow and high turbidity.

5.4. Storms

When storms pass through the study area, they block the normal trade winds, causing strong winds from other orientations (usually the south), and bring large waves, resulting in flow that has characteristics that are a mix of relaxation events and large waves (Fig. 7). Similar to relaxation events, the currents up in the water column over the fore reef were asymmetric to the northwest and alongshore flow to the southwest, even during falling tides, was rarely observed. Flows close to the bed over the fore reef and on the reef flat were directed offshore, however, and were similar to those observed under large wave conditions; mean flux also showed similar orientations.

5.5. Implications of transport patterns to reef processes

The spatial, both horizontally across the reef and vertically through the water column, and temporal differences in the magnitude and direction of currents and turbidity flux demonstrate the complexity of flow and the transport of turbid water along a relatively geometrically simple fringing reef. At a given location on the reef, there is substantial vertical variability in current orientation, with flow directions and the resulting turbidity flux often varying by more than 90° in the relatively shallow ($\sim$10 m) water column (Fig. 7). Thus, material distributed throughout the water column, including the particles in suspension causing the turbidity (e.g. sediment or larvae) and/or dissolved nutrients and contaminants, under constant oceanographic and meteorologic forcing, could be

transported in different directions. Furthermore, under constant forcing, the transport of material at the same height above the seafloor would be different at different locations across the reef depending on the water depth, similar to the observations made by Roberts et al. (1992) in the Caribbean. The data presented here, however, suggest that off western Maui the delineations made by Roberts et al. (1992) between wave-dominated and current-dominated regions of a fringing reef are not just based on location across the reef, but vary temporally and vertically in the water column.

The temporally- and spatially-varying nature of flow and flux has implications for both biologic and geologic processes. Kolinski and Cox (2003) show that 71% of broadcast spawning corals in Hawaii display peak gamete or planula release during the summer (June-September) when the flows over the fringing reef off northwest Maui are dominated by trade wind conditions. This would imply that larvae spawned from the reefs in the study area would likely be carried offshore and downwind by the prevailing currents, similar to the observations made by Storlazzi et al. (2006a) during the 2003 summer spawning season. While this would not result in seeding of the natal reef, it would circulate larvae within the islands of Maui, Molokai, and Lanai, increasing the supply and diversity of larvae to the reefs on adjacent islands downstream from the study area. The summer spawning period is also characterized by the high-frequency internal bores, which may help to bring settling larvae back onshore into suitable water depths or habitat to settle and recruit. However, these same bores also have the potential to advect nutrient or contaminant-laden deep injection well water (Soicher and Peterson, 1996; West Maui Watershed Management Project, 1996; Dollar and Andrews, 1997) that has percolated out of the island at depth up onto the reefs during this biologically important period.

While the largest delivery of sediment and potential contaminants by fluvial discharge or overland flow is greatest during the winter when rainfall is highest, the processes of transport over the fringing reef off Kahana decrease the impacts of these inputs. The large wave stresses and strong offshore flow over the reef flat during winter storms and large wave events would resuspend the relatively fine-grained, slowly-settling sediment deposited on the reef flat from terrestrial sources and transport it offshore (Fig. 7), possibly in a nepheloid layer similar to that observed by Wolanski et al. (2003). These same large wave stresses and the strong offshore flows throughout the water column over the fore reef would limit the deposition and thus the impact of the fine-grained terrestrial sediment on the corals on the fore reef by advecting it quickly offshore beyond the fore reef system.

Further evidence of offshore transport of fine-grained terrestrial sediment derives from sediment traps attached to both the fore reef and reef flat instrument packages during the last deployment. The high percentage (>68%) of the fine-grained material being terrigenous in origin found in both traps (as discussed in Section 4.2) but not observed on the surrounding seabed suggest that, while the energetics of the environment are generally too great to allow for the long-term deposition of terrestrial fine-grained silts and clays on the seabed, large quantities of fine-grained terrigenous sediment move through the study area. Because sediment traps generally under-sample slowly-settling, fine-grained material in energetic environments (e.g. Gardner et al., 1983), we interpret the high percentage of fine-grained terrestrial material in both the reef flat and fore reef traps to mean that there are large quantities of terrestrial fine-grained sediment moving through the system. Thus, while not observed on the seabed during low-energy conditions or incorporated in the geologic record, this terrigenous sediment is advected over the reef, potentially decreasing photosynthetically-available radiation (PAR) and possibly desorbing nutrients (De Carlo and Dollar, 1997) and/or contaminants.

The transport of turbid water over the fringing reef is highly seasonal. Over the course of a year, the majority of the turbidity flux occurred during the trade wind-dominated summer period (Fig. 8). While turbidity is greatest during large wave events and storms, the low frequency of these conditions results in lower net flux than the lower-energy, but much more frequent, trade wind conditions. The moderately high turbidity levels on the reef flat during the spring and summer when trade winds dominate the forcing is likely caused by the resuspension of sediment deposited on the inner reef flat by fluvial discharge that generally occurs in the winter; this sediment is then transported downwind to the southwest, with limited exchange between the reef flat and fore reef. The daily increases and decreases in wind-driven current and wind-driven wave stresses, in conjunction with the phasing of these stresses and tidal elevation, appears to result in some sediment being resuspended and then settling out each day (as inferred from rhythmic turbidity levels) on the reef flat as it is transported downwind along the reef flat. This repetitive resuspension and deposition likely increases the relative impact of this sediment on biologic processes, since a given sediment particle might be resuspended, causing turbidity and decreasing PAR, then re-deposited on a coral each day. This probably causes physiologic stress or at least a decrease in usable energy as the coral receives reduced PAR and diverts energy for mucus production to slough off the settling sediment (Fabricius, 2005).

Fine-grained terrestrial material, which was collected in both the reef flat and fore reef sediment traps, is of concern because its dark color and low settling velocity means that it tends to stay in suspension for long periods of time and thus block the incident PAR needed by the symbiotic photosynthetic algae in the corals. Resuspension of coarser bed material on the reef flat appears to be limited to periods of concurrent high tides, large waves and strong trade winds when combined wave-current shear stresses are high; the net transport of this material on the reef flat is limited due to its high settling velocity and the shorter period of resuspension. Near-bed flows over the fore reef under all sets of conditions were offshore; this offshore-directed bottom flow may be balancing wave- and wind-driven onshore surface flow in a thin surface layer and may represent the mechanism by which the reef sheds material generated by bioerosion and mechanical abrasion of corals and coralline algae.

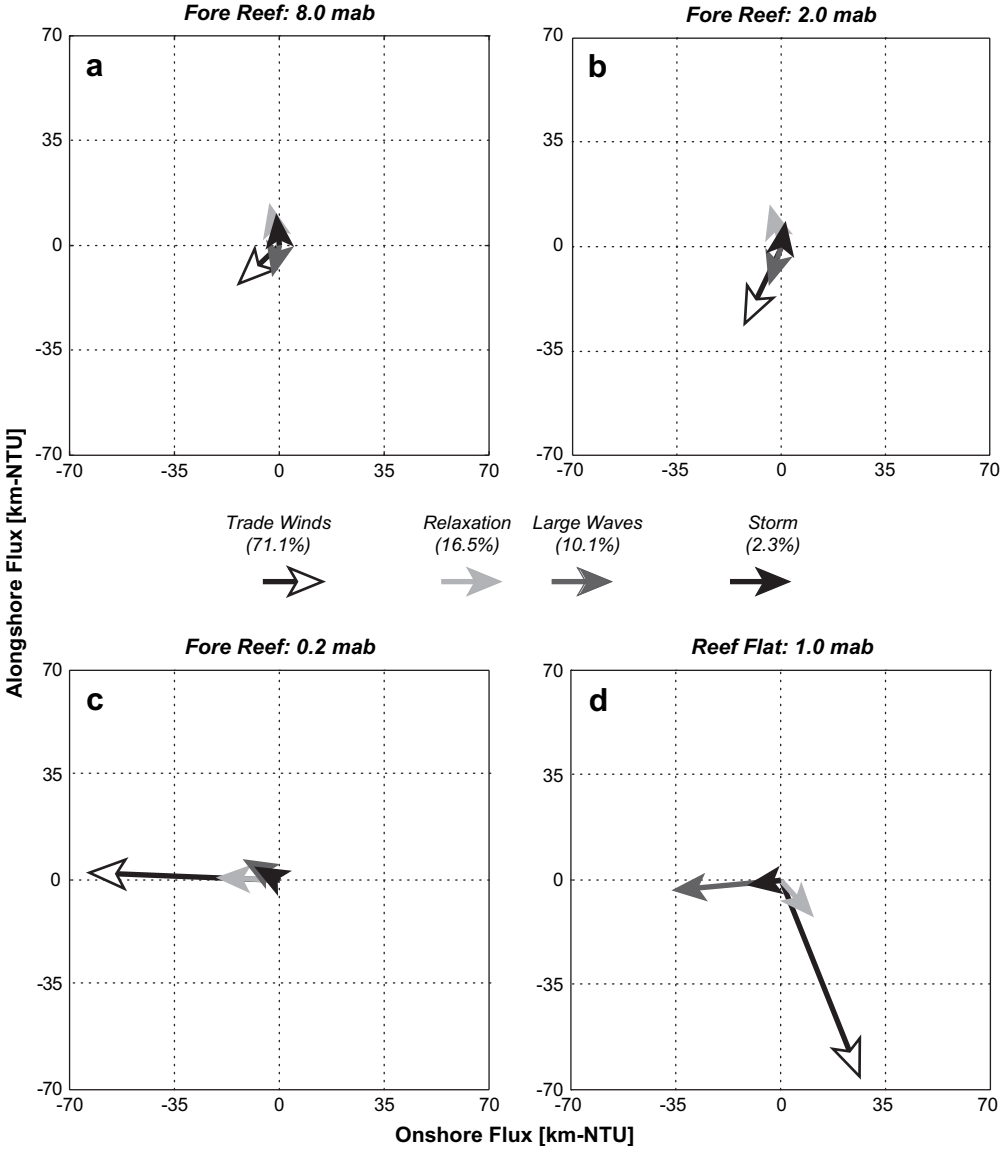

Fig. 8. Variability in net turbidity flux, calculated as the cumulative product of the current velocity and turbidity over the duration of each of the four combinations of meteorologic and oceanographic forcing defined in Fig. 7, for different location across the reef and at different depths. (a) Fore reef at 8.0 mab. (b) Fore reef at 2.0 mab. (c) Fore reef at 0.2 mab. (d) Reef flat at 1.0 mab. Positive alongshore is defined upwind to the northeast and the units are: km-NTU. The percentages represent the frequency distribution of these different sets of conditions over the 12-month period between February 2002 and February 2003, when the data coverage was greatest. Note that net turbidity flux is almost always offshore on the fore reef, especially close to the seafloor, and net flux both on the reef flat and over the fore reef is dominated by the persistent trade wind forcing.

Overall, under these four combinations of meteorologic and atmospheric forcing, velocity shear, both vertically through the water column and horizontally across the reef, was observed. This shear results in different magnitudes and directions of flow and the transport of turbid water, highlighting the extremely complex nature of flow over a relatively geometrically simple fringing reef. These findings suggest that sampling protocols and field experiments need much greater spatial and temporal resolution to reflect the true range of variability in flow, water column properties, and the transport of turbid water over a fringing reef than along less complex, sandy shorelines where flow features are often coherent over length scales an order of magnitude greater. Furthermore, while the relative contribution of these different combinations of meteorologic and atmospheric forcing may vary from reef to reef, since the majority of the world's coral reefs lie within the northern and southern hemispheres' trade wind belts (Spalding et al., 2001), the general mechanisms and patterns described here likely characterize a wide range of fringing reefs around the world.

6. Conclusions

The data presented here detail how flow and water column properties vary over a fringing reef over time scales ranging from minutes to seasons and are driven by waves, winds, tides and internal bores. Four sets of meteorologic and oceanographic

conditions were defined that control the spatial and temporal variability in flow and transport over the fore reef and reef flat at Kahana, northwest Maui. Throughout the period of study, near-surface current directions over the fore reef varied on average by more than 41° from those near the seafloor, and the orientation of the currents over the reef flat differed on average by more than 65° from those observed over the fore reef. The late spring, summer, and early fall were characterized by low wave energy and relative consistent trade wind forcing. During this time, which encompasses the coral spawning season, there was downwind transport on the fringing reef, punctuated by upwind flow during periods of weak winds or reversals in wind direction. Internal bores were frequently observed during this time. During the energetic winter months, turbidity was much greater and flow throughout most of the water column, both over the fore reef and on the reef flat, was oriented offshore. While turbidity is greatest during large wave events and storms, the low frequency of these conditions results in lower annual flux on the fringing reef than the lower-energy, but much more frequent, trade wind conditions that typify the late spring, summer, and early fall. These observations demonstrate the high spatial variability in flow and the transport of turbid water across a relatively geometrically-simple fringing reef. Only by understanding the natural variability of these parameters over the range of seasons that characterize an area can one design sampling schemes that will be representative of the annual budget of the system, or conversely, put the limited measurements typically made in the context of the total variability of the system.

Acknowledgments

This work was carried out as part of the U.S. Geological Survey's Coral Reef Project as part of an effort in the United States and its trust territories to better understand the effects of geologic processes on coral reef systems. We would like to thank Project Chief Mike Field, whose support made it possible to conduct such an extensive field experiment. Eric Brown (NPS), John Gorman, Jim Luecke and Fred Putnam (Maui Ocean Center) went out of their way to help us carry out this experiment and for that we owe them great thanks. We would also like to thank Jodi Eshleman (USGS), Kurt Rosenberger (USGS), and Eric De Carlo (UH), who contributed numerous excellent suggestions and a timely review of our work. Use of trademark names does not imply USGS endorsement of products.

References

Acevedo, R.J., Morelock, J., Olivieri, R.A., 1989. Modification of coral reef zonation by terrigenous sediment stress. Palios 4, 92–100.

Bothner, M.H., Reynolds, R.L., Casso, M.A., Storlazzi, C.D., Field, M.E., 2006. Quantity, composition and source of sediment collected in sediment traps along the fringing coral reef off Molokai, Hawaii. Marine Pollution Bulletin 52 (9), 1034–1047.

Buddemeir, R.W., Hopley, D., 1988. Turn-ons and turn-offs: causes and mechanisms of the initiation and termination of coral reef growth. Proceedings of the 6th International Coral Reef Congress, 253–261.

Clague, D.A., Dalrymple, G.B., 1989. Tectonics, geochronology, and origin of the Hawaiian Emperor Volcanic chain. In: Winterer, E.L., Hussong, D.M., Decker, R.W. (Eds.), The Eastern Pacific Ocean and Hawai'i. The Geological Society of America, Boulder, CO, pp. 188–217.

De Carlo, E.H., Dollar, S.J., 1997. Assessment of Suspended Solids and Particulate Nutrient Loading to Surface Runoff and the Coastal Ocean in the Honokowai Drainage Basin, Lahaina District, Maui. Final report to NOAA/Algal Blooms Project and Hawaii State DOH, 32.

Deines, K.L., 1999. Backscatter estimation using broadband acoustic Doppler current profilers. RD Instruments Application Note FSA-008, 5 pp.

Devlin, M.J., Lourey, M.J., 2000. Water Quality—Field and Analytical Procedures. Long-term Monitoring of the Great Barrier Reef, Standard Operating Procedure Number 6. Australian Institute of Marine Sciences, Townsville, 36 pp.

Dollar, S., Andrews, C., 1997. Algal blooms off West Maui: Assessing Casual Linkages Between Land and the Coastal Ocean. Final Report. University of Hawaii, Honolulu, Hawaii, 40 pp.

Fabricius, K.E., 2005. Effects of terrestrial runoff on the ecology of corals and coral reefs: review and synthesis. Marine Pollution Bulletin 50, 125–146.

Flament, P., Lumpkin, C., 1996. Observations of currents through the Pailolo Channel: Implications for nutrient transport. In: Wiltse, W. (Ed.), Algal Blooms: Progress Report on Scientific Research. West Maui Watershed Management Project, pp. 57–64.

Fletcher, C.H., Richmond, B.M., Grossman, E.E., Gibbs, A.E., 2002. Atlas of Natural Hazards in the Hawaiian Coastal Zone. USGS Geologic Investigations Series I-2716.

Fortes, M., 2000. The effects of siltation on tropical coastal ecosystems. In: Wolanski, E. (Ed.), Oceanographic Processes of Coral Reefs. CRC Press, Boca Raton, pp. 93–112.

Gardner, W.D., Richardson, M.J., Hinga, K.R., Biscaye, P.E., 1983. Resuspension measured with sediment traps in a high-energy environment. Earth and Planetary Science Letters 66, 262–278.

Gibbs, A.E., Grossman, E.E., Richmond, B.M., 2005. Summary and preliminary interpretations of USGS cruise A202HW: Underwater video surveys collected off Oahu, Molokai and Maui, Hawaii, June–July, 2002. U.S. Geological Survey Open-File Report 2005-1244, 57.

Gourlay, M.R., 1996. Wave set-up on coral reefs. 1. Set-up and wave-generated flow on an idealized two dimensional horizontal reef. Coastal Engineering 27, 161–193.

Holdaway, G.P., Thorne, P.D., Flatt, D., Jones, S.E., Prandle, D., 1999. Comparison between ADCP and transmissometer measurements of suspended sediment concentration. Continental Shelf Research 19, 421–441.

Jokiel, P.L., Brown, E.K., Friedlander, A., Rodgers, S.K., Smith, W.R., 2001. Hawaii Coral Reef Initiative Coral Reef Assessment and Monitoring Program (CRAMP) Final Report 1999–2000. University of Hawaii, Hawaii, 66 pp.

Kolinski, S.P., Cox, E.F., 2003. An update on modes and timing of gamete and planula release in Hawaiian Scleractinian corals with implications for conservation and management. Pacific Science 57, 17–27.

Kraines, S.B., Yanagi, T., Isobe, M., Komiyama, H., 1998. Wind-wave driven circulation on the coral reef at Bora Bay, Miyako Island. Coral Reefs 17, 133–143.

Larcombe, P.A., Ridd, P.V., Prytz, A., Wilson, B., 1995. Factors controlling suspended sediment on inner-shelf coral reefs, Townsville, Australia. Coral Reefs 14, 163–171.

Leichter, J.L., Stewart, H.L., Miller, S.L., 2003. Episodic nutrient transport to Florida coral reefs. Journal of Limnology and Oceanography 48 (4), 1394–1407.

Lowe, R.J., Falter, J.L., Bandet, M.D., Pawlak, G., Atkinson, M.J., Monismith, S.G., Koseff, J.R., 2005. Spectral wave dissipation over a barrier reef. Journal of Geophysical Research 110, C04001. doi:10.1029/2004JC002711.

Lugo-Fernandez, A., Roberts, H.H., Wiseman, W.J., Carter, B.L., 1998. Water level and currents of tidal and infragravity periods at Tague Reef, St. Croix (USVI). Coral Reefs 17, 343–349.

Marszalek, D.S., 1981. Impact of dredging on a subtropical reef community: Southeastern Florida, U.S.A. Proceedings of the 4th International Coral Reef Congress, 147–153.

Pacific, M&E, 1991. Water Use and Development Plan for the Island of Maui, 1992. Draft report prepared for the Department of Water Supply. County of Maui, Hawaii.

Merrifield, M.A., Yang, L., Luther, D.S., 2002. Numerical simulations of a storm generated island-trapped wave event at the Hawaiian Islands. Journal of Geophysical Research 107 (C10), 3169. doi:10.1029/2001JC001134.

Moberly, R.M., Chaimberlin, T., 1964. Hawaiian Beach Systems. University of Hawaii, Hawaii.

National Climate Data Center, National Oceanographic and Atmospheric Administration, 2004. NCDC hourly surface climate data for Hawaii, online, dataset. 276 KB. http://www.ncdc.noaa.gov/oa/climate/climatedata.html#hourly.

Ogston, A.S., Storlazzi, C.D., Field, M.E., Presto, M.K., 2004. Currents and suspended sediment transport on a shallow reef flat: South-central Molokai, Hawaii. Coral Reefs 23, 559–569.

Osborne, P.D., Vincent, C.E., Greenwood, B., 1994. Measurement of suspended sand concentrations in the nearshore: field comparison between optical and acoustic backscatter sensors. Continental Shelf Research 14 (2/3), 159–174.

Pinkel, R., Munk, W., Worcester, P., Cornuelle, B.D., Rudnick, D., Sherman, J., Filloux, J.H., Dushaw, B.D., Howe, B.M., Sanford, T.B., Lee, C.M., Kunze, E., Gregg, M.C., Miller, J.B., Moum, J.M., Caldwell, D.R., Levine, M.D., Boyd, T., Egbert, G.D., Merrifield, M.A., Luther, D.S., Firing, E., Brainard, R., Flament, P.J., Chave, A.D., 2000. Ocean mixing studied near Hawaiian Ridge. EOS 81 (46), 545, 553.

Presto, M.K., Ogston, A.O., Storlazzi, C.D., Field, M.E., 2006. Temporal and spatial variability in the flow and dispersal of suspended-sediment on a fringing reef flat, Molokai, Hawaii. Estuarine, Coastal and Shelf Science 67, 67–81.

Reichel, G., Nachtnebel, H.P., 1994. Suspended sediment monitoring in a fluvial environment: Advantages and limitations of applying an acoustic Doppler current profiler. Water Research 28 (4), 751–761.

Roberts, H.H., Murray, S.P., Suhayda, J.N., 1980. Physical processes in a fringing reef system. Journal of Marine Research 33, 233–260.

Roberts, H.H., Wilson, P.A., Lugo-Fernandez, A., 1992. Biologic and geologic responses to physical processes: examples from modern reef systems of the Caribbean-Atlantic region. Continental Shelf Research 12 (7/8), 809–834.

Rogers, C.S., 1990. Responses of coral reefs and reef organisms to sedimentation. Marine Ecology Progress Series 62, 185–202.

Soicher, A.J., Peterson, F.L., 1996. Assessing Terrestrial Nutrient and Sediment Discharge to the Coastal Waters of West Maui, Hawaii. University of Hawaii, Honolulu, Hawaii, 98 pp.

Spalding, M.D., Ravilious, C., Green, E.P., 2001. World Atlas of Coral Reefs. United Nations Environmental Program, World Conservation Monitoring Center, Cambridge, England, 424 pp.

State of Hawaii, 2004. Department of Health Administrative Rules, Water Quality Standards, Chapter 54, Title 11. Hawaii, Honolulu, 62 pp.

Storlazzi, C.D., Jaffe, B.E., 2003. Coastal Circulation and Sediment Dynamics along West Maui, Hawaii, PART I: Long-term measurements of currents, temperature, salinity and turbidity off Kahana, West Maui: 2001–2003. U.S. Geological Survey Open-File Report 03-482, 28.

Storlazzi, C.D., Ogston, A.S., Bothner, M.H., Field, M.E., Presto, M.K., 2004. Wave- and tidally-driven flow and sediment flux across a fringing coral reef: South-central Molokai, Hawaii. Continental Shelf Research 24 (12), 1397–1419.

Storlazzi, C.D., Brown, E.K., Field, M.E., 2006a. The application of acoustic Doppler current profilers to measure the timing and patterns of coral larval dispersal. Coral Reefs 25, 369–381.

Storlazzi, C.D., McManus, M.A., Logan, J.B., McLaughlin, B.E., 2006b. Cross-shore velocity shear, eddies and heterogeneity in water column properties over fringing coral reefs: West Maui, Hawaii. Continental Shelf Research 26, 401–421.

Tartinville, B., Rancher, J., 2000. Wave-induced flow over Mururoa Atoll reef. Journal of Coastal Research 16 (3), 776–781.

Thorne, P.D., Vincent, C.E., Hardcastle, P.J., Rehman, S., Pearson, N., 1991. Measuring suspended sediment concentrations using acoustic backscatter devices. Marine Geology 98, 7–16.

Western Region Climate Center, 2006. Historical climate information, online edition. http://www.wrcc.dri.edu/narratives/HAWAII.htm.

West Maui Watershed Management Project, 1996. Algal Blooms: Progress Report on Scientific Research. West Maui Watershed Algal Bloom Task Force, Maui, Hawaii, 64.

Wolanski, E., Marshall, K., Spagnol, S., 2003. Nepheloid layer dynamics in coastal waters of the Great Barrier Reef. Journal of Coastal Research 19 (3), 748–752.

Wolanski, E., Delesalle, B., 1995. Upwelling by internal waves, Tahiti, French Polynesia. Continental Shelf Research 15 (2/3), 357–368.